Available online at www.sciencedirect.com
ScienceDirect
Journal of Power Sources 171 (2007) 218–223
JOURNAL OF POWER SOURCES
www.elsevier.com/locate/jpowsour

Short communication

Nanoimprinted electrodes for micro-fuel cell applications☆

André D. Taylor[a,*], Brandon D. Lucas[b], L. Jay Guo[b,c], Levi T. Thompson[a,b]

[a] *Department of Chemical Engineering, University of Michigan, United States*
[b] *Applied Physics, University of Michigan, United States*
[c] *Electrical Engineering and Computer Science, Macromolecular Science and Engineering, University of Michigan, United States*

Received 15 September 2006; received in revised form 8 January 2007; accepted 13 January 2007
Available online 20 January 2007

Abstract

Nanoimprint lithography (NIL) was used to fabricate electrodes with high specific Pt surface areas for use in micro-fuel cell devices. The Pt catalyst structures were characterized electrochemically using cyclic voltammetry and were found to have electrochemical active surface areas (EAS) ranging from 0.8 to 1.5 $m^2\ g^{-1}$ Pt. These NIL catalyst structures were tested in fuel cell membrane electrode assemblies (MEA) by directly embossing a Nafion 117 membrane. The features of the mold were successfully transferred to the Nafion and a 7.5 nm thin film of Pt was deposited at a wide angle to form the anode catalyst layer. The resulting MEA yielded a very high Pt utilization of 15,375 mW mg^{-1} Pt compared to conventionally prepared MEAs (820 mW mg^{-1} Pt). Embossing pattern transfer was also demonstrated for spin casted Nafion films which could be used for new applications.

Keywords: Nanoimprint lithography; Micro-fuel cell; Electrode; Thin film catalyst; Nafion; Embossing

1. Introduction

Fuel cells are an attractive alternative to batteries for portable electronic devices. Micromachining methods hold promise for producing fuel cell structures with high degrees of materials utilization and low costs. Several approaches have been reported for the production of micro-fuel cells using micromachining techniques [1–4]. Most of these devices include micromachined fuel cell components combined with conventional macro-MEAs (membrane electrode assemblies). Morse et al. [5] and Taylor and Thompson [6] recently demonstrated micro-fuel cells with most of the components produced using micromachining methods. Catalyst structures produced via electrodeposition of Pt and Pd have also been demonstrated in a micro-fuel cell [7].

Towards improving the performance and lowering the cost of the electrodes, we report the use of nanoimprint lithography (NIL) to fabricate electrodes with high specific Pt surface areas. Nanoimprint lithography is an emerging lithographic technology that has applications for high-throughput patterning of nanostructures [8]. Based on the mechanical embossing principle, nanoimprint techniques can achieve pattern resolutions beyond the limitations set by light diffraction or beam scattering in other conventional techniques [8,9]. In addition, NIL can be used to pattern nonflat surfaces without the need for planarization [10]. In this article, we report methods for using NIL to create fuel cell electrodes. We will also demonstrate methods to use NIL to emboss nanostructures onto spin casted Nafion films as well as bulk Nafion 117. For the Nafion 117, a shadow mask was used and a thin film of Pt catalyst was deposited on top of the nanostructures at a wide angle which prevented the formation of a continuous film. This Nafion film was then incorporated into an MEA and evaluated in a fuel cell. To our knowledge, this is the first time this technique has been demonstrated for fuel cell applications.

2. Experimental materials/methods

2.1. Fabrication

Fabrication of the electrodes and all of the nanoimprinting processes were conducted in the Michigan Nanofabrication Facility. Fig. 1 illustrates the standard NIL process [9].

☆ Special Issue Oral Presentation from Fuel Cells Science and Technology Conference, 13–14 September 2006, Turin, Italy.

* Corresponding author at: University of Michigan, 3142 H.H. Dow Building, 2300 Hayward Street, Ann Arbor, MI 48109-2136, United States.
Tel.: +1 734 763 5771; fax: +1 734 763 0459.
E-mail address: adtaylor@umich.edu (A.D. Taylor).

0378-7753/$ – see front matter © 2007 Published by Elsevier B.V.
doi:10.1016/j.jpowsour.2007.01.026

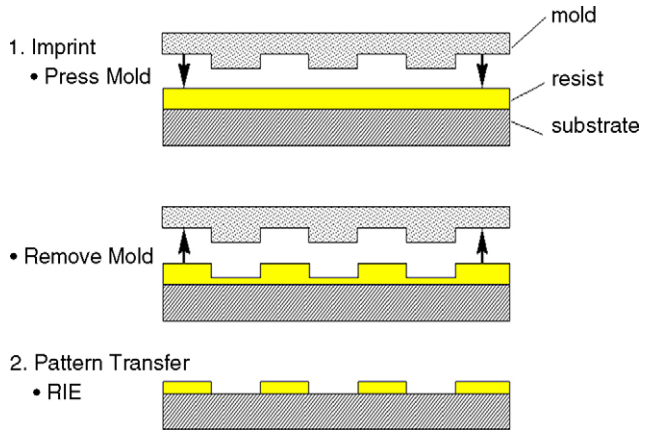

Fig. 1. Nanoimprint lithography process.

2.2. Nanoimprint molds

The one-dimensional SiO_2 grating mold used for electrode fabrication and Nafion embossing is characterized by a 1:1 duty cycle and 700 nm pitch. The flexibility of the NIL technique permits the simultaneous transfer of nanoscale features to a variety of different substrates. Fig. 2 illustrates SiO_2 molds that we have used for nanoimprinting. Results reported in this paper used the mold illustrated in Fig. 2A.

2.3. Nanoimprinted electrodes

The nanoimprinted electrodes were fabricated on a single side polished P type 4 in. ⟨1 0 0⟩ silicon wafer. Following a standard pre-furnace clean, a 200 nm low pressure chemical vapor deposition (LPCVD) oxide was grown on the wafer to isolate the electrodes from the substrate. A 200 nm planar Au film was deposited using an electron beam (e-beam) evaporator (Enerjet Evaporator, pressure $< 10^{-6}$ Torr) with a 3 nm Ti underlayer serving as an adhesion promoter. The wafers were then cleaved to appropriate sizes for the nanoimprint lithography step.

2.4. Nanoimprint lithography

The nanoimprint resist (Micro Resist Technology mr-I 8030; $T_g = 115\,^{\circ}C$) was spin cast (250 nm) onto the freshly prepared substrate and baked using a hotplate (140 °C; 5 min) to remove residual solvent. The sample was then imprinted using a custom-built nanoimprinter (700 psi, 180 °C, 5 min), cooled to 55 °C and released from the mold. An electron beam deposited Cr mask layer was applied to the protruding lines of the surface relief pattern using shadow evaporation at approximately 60° off normal. This step was included to help increase the fidelity of pattern transfer during residual polymer removal independent of the etch anisotropy and to create preferred undercut for liftoff processing. The residual polymer layer was removed using (RIE) reactive-ion etching (20 sccm O_2, 50 W, 20 mT).

The Pt catalyst lines (5–200 nm) were subsequently deposited using e-beam evaporation onto a 3 nm Ti adhesion layer through a shadow mask to produce a well-defined rectangular nanostructured surface. Metal and resist liftoff were accomplished using an acetone soak and gentle mechanical cleaning with a swab was used to remove any residual insoluble complex from the Pt and Au surfaces. Fig. 3A illustrates an electrode with Pt nanobars (thickness: 50 nm) shown in the blue region which covered an active area of 13 mm × 4 mm. Fig. 3B illustrates two electrodes fabricated on the same substrate. Both electrodes were electrically isolated and were used to verify the reproducibility of the shadow masks. The area of the shadow masks for these electrodes corresponds to a Pt area of 4.5 mm × 4.5 mm and thickness of 5 nm. The contrast in color for the electrodes corresponds to light diffracted at different angles due to the grating pattern of the imprinted regions. Fig. 4 is a

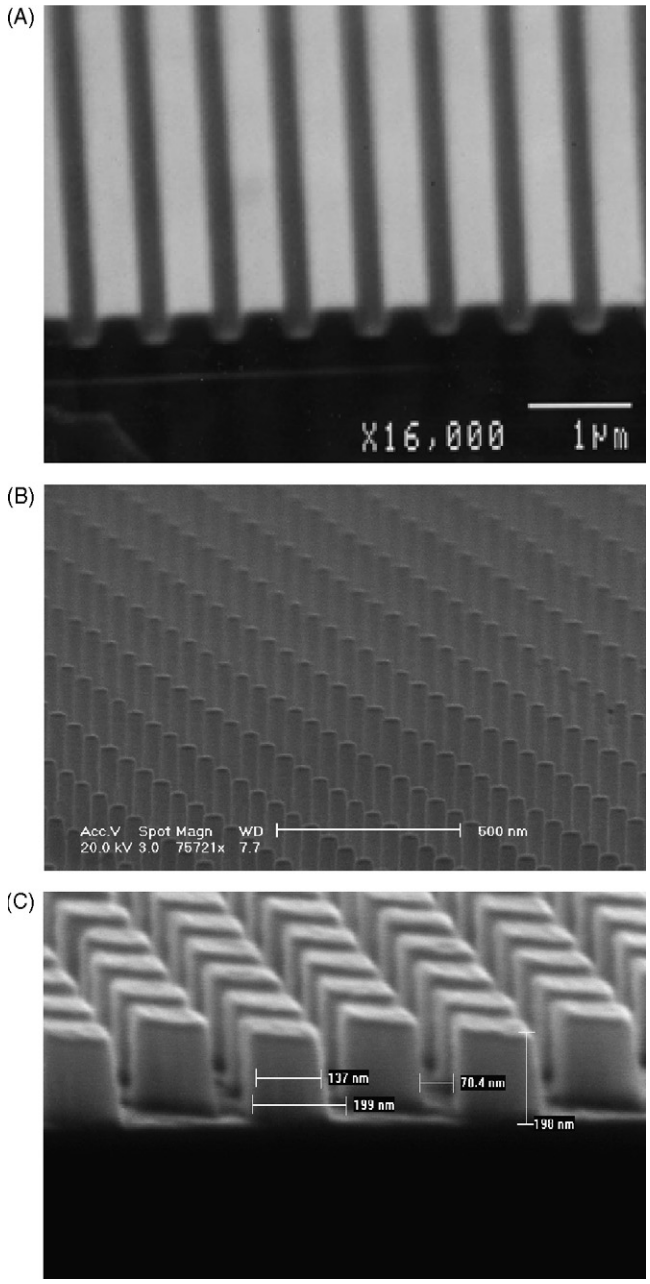

Fig. 2. (A) SEM image of grating mold structure (1:1 duty cycle 700 nm period); (B) rod mold structure; (C) cube mold structure.

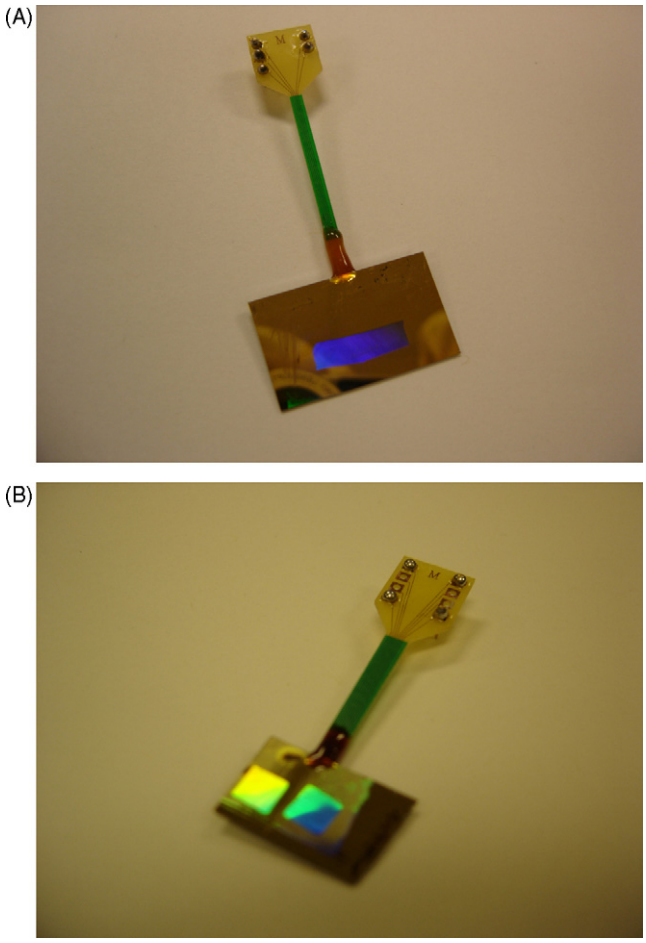

Fig. 3. (A) Pt nanostructured electrode 13 mm × 4 mm; (B) 2 Pt nanostructured electrodes 4.5 mm × 4.5 mm.

scanning electron micrograph (SEM) of the Pt nanoimprinted electrodes. The width and pitch of the bars were determined to be 350 nm which corresponds to the 700 nm period grating mold (Fig. 2A). The full dimensions of a single Pt bar in Fig. 3A and B are 13 mm × 350 nm × 50 nm, and 4.5 mm × 350 nm × 5 nm, respectively.

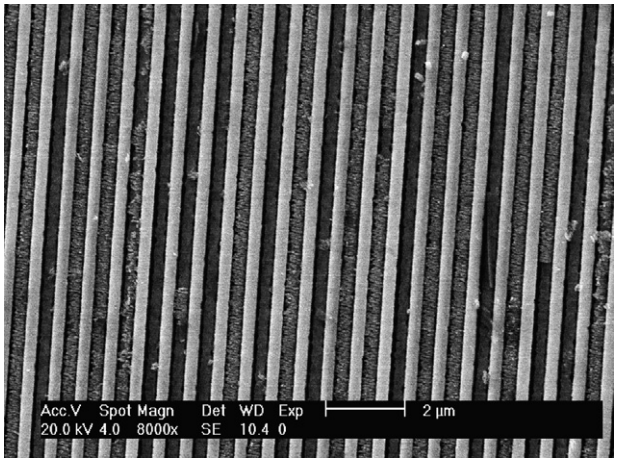

Fig. 4. SEM image of the Pt nanoimprinted electrodes.

2.5. Spin cast Nafion embossing

Nafion solutions (5% Aldrich) were spin cast onto pieces of oxide covered silicon. The thickness of the film was 500 nm and was calibrated at a spin speed of 500 rpm. The molds were pressed into the substrates at 900 psi and 135 °C for 5 min. These conditions yielded the best transfer of mold features to the thin films. Fig. 5 illustrates results from embossing a Nafion thin film. The colored region identifies the imprinted sample area which is held at different angles to demonstrate light diffraction. The pattern transferred to these features was very uniform. Fig. 6 shows an SEM cross-section of the imprinted Nafion film.

2.6. Nafion 117 embossing

The Nafion 117 films were cleaned using procedures that we have successfully used in the past. To remove organic impurities and to obtain the H^+ form for use in the PEM fuel cell, the membranes were pretreated by boiling the pieces in 50 vol.% HNO_3 and deionized water for 1 h. The films were then rinsed in boiling deionized (DI) water for 30 min, boiled in a 0.5 M H_2SO_4 solution for 30 min, and boiled twice in DI water for 30 min. The membranes were subsequently stored in DI water until ready for use.

A hydrated Nafion 117 membrane was placed onto a clean Si substrate and dried using a stream of N_2 to remove any visually observable water droplets from the surface. The mold was then placed directly onto the membrane and inserted into the nanoimprinter chamber. A pressure of 900 psi was immediately applied to the sample to minimize membrane buckling due to loss of moisture as the chamber temperature was increased to 150 °C. The film was held at 150 °C for 5 min then cooled to 55 °C. The mold was separated from the membrane and a thin film of Pt (7.5 nm) was deposited onto the protruding lines of the embossed pattern. A shadow mask was used to ensure that the Pt was deposited only on the embossed region, and the film was oriented at an angle from the Pt target to maximize Pt coverage on the peaks and valleys of the embossed (nanostructured) region.

2.7. Electrode characterization

The catalyst structures (fabricated on gold covered SiO_2 on silicon; Figs. 3 and 4) were characterized electrochemically using cyclic voltammetry in a half-cell three electrode system containing 0.5 M H_2SO_4 electrolyte versus a Ag/AgCl reference electrode (Bio Analytic Systems). The electrolyte solutions were prepared from Milli-Q® water and sulfuric acid (Fischer CMOS grade). Prior to carrying out an experiment the electrolyte in the three-electrode chemical cell was purged with Argon for 30 min. The electrode potential was controlled by a PAR (Prince Applied Research) Model 273 potentiostat which was controlled using CorrWare Electrochemical Experiment Software developed by Scribner Associates, Inc. The counter electrode was a Pt wire attached to a Pt mesh. Potentials are quoted versus the Ag/AgCl reference electrode. Before each experiment the counter and working electrodes were thoroughly rinsed in Milli-Q® water.

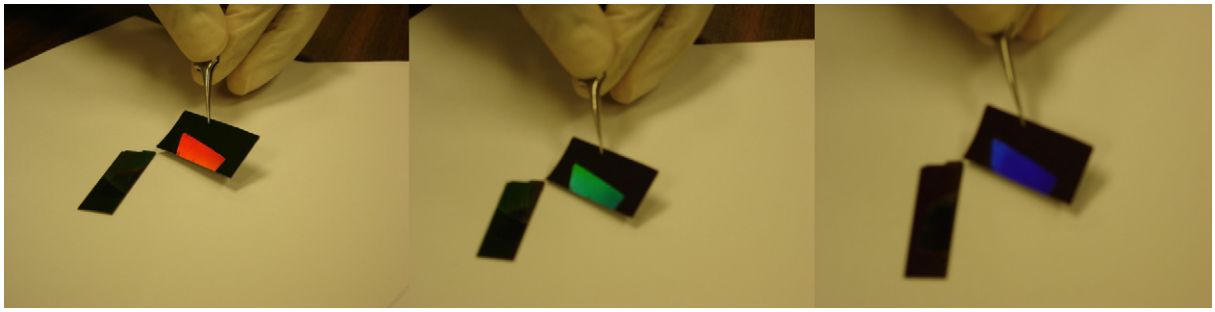

Fig. 5. Nanostructured Nafion thin film.

2.8. Fuel cell tests

Membrane electrode assemblies incorporating the standard electrode and the embossed Nafion 117 anode side with a Pt thin film were fabricated using E-tek (ELAT V3.1 double side automated) gas diffusion layers (GDLs). The catalyst ink solutions were prepared using a Johnson Matthey Pt/C catalyst (20 wt.% Pt loading). The cathode catalyst layers with Pt loadings of 0.5 mg cm^{-2} were prepared using an ink solution consisting of 68% Pt/C, 20% Nafion, and 12% PTFE by weight. The standard MEA anode consisted of 75% Pt/C and 25% Nafion with a Pt loading of 0.5 mg cm^{-2}. The nanoimprinted MEA had a Pt anode loading of 8.0 μg cm^{-2} and a standard cathode. The MEAs were fabricated by hot pressing the electrolyte membrane between two GDLs at 135 °C for 5 min at a pressure of 10 MPa. The MEAs were tested in a single fuel cell housing. The MEAs were conditioned overnight until a steady state current was achieved at a potential of 0.6 V. The temperature of the fuel cell was 80 °C and the anode and cathode saturators were set at 90 °C which yield reactant gases with 100% relative humidity. The flow rates of the humidified hydrogen and oxygen were held constant at 100 sccm using mass flow controllers.

3. Results

A characteristic voltammogram for the nanoimprinted electrode on SiO_2 (on silicon) is presented in Fig. 7. The features are typical of polycrystalline Pt. The thickness of the Pt layer was 50 nm based on on-line monitoring using a frequency-shift measurement from a resonating crystal. The hydrogen desorption region was integrated to determine the coulombic charge (corrected for the double-layer capacitance of the Pt and Au/Ti support) for each electrode and yielded a maximum electrochemical active surface (EAS) area of 1.5 m^2 g^{-1} Pt. These EAS values are higher than those for micro-fuel cell electrodes we previously reported [6]. Our previous electrodes were prepared using standard micromachining methods and typically had EAS areas of ∼0.3 m^2 g^{-1} Pt. These EAS areas are lower than those for typical fuel cell catalysts which range from 65 to 100 m^2 g^{-1} for lower-loaded catalysts (e.g. 20 wt.% Pt/Vulcan XC72) [11]. The EAS areas for electrodes produced using the NIL method will be improved with further development.

Figs. 5 and 6 demonstrate the results of imprinting nanostructures directly onto Nafion thin films. The features possess a distinct 700 nm period. The surface edges of the embossed film appeared to be rounded which suggests that the films relaxed (and/or expanded) after the compression step. This may be due to the fact that the films were embossed immediately after casting without curing. The consistent color diffraction in the imprinted region suggests that the rest of the film was not compromised from this process. The embossing of nanostructures onto Nafion thin films holds promise for a variety of new micro-fuel cell designs. In addition, micro-fluidic devices that exploit the proton selectivity of Nafion for reactions and/or separations could be possible. We are presently investigating the viability of these options.

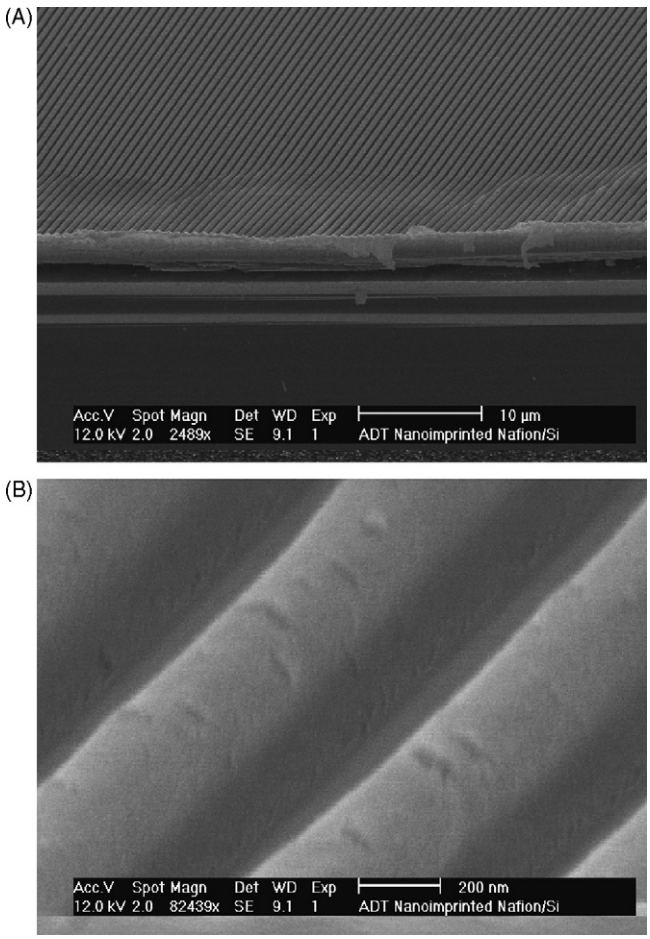

Fig. 6. (A) SEM cross-section of Nafion® nanostructured thin film; (B) enlarged SEM cross-section of Nafion® nanostructured thin film.

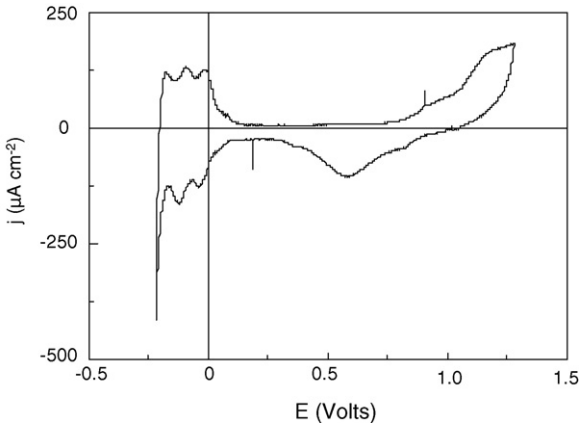

Fig. 7. Cyclic voltammogram of Pt nanostructured electrode.

The embossing of Nafion 117 is a fairly simple process. Our earlier attempts focused on casting a uniform layer of nanoimprint resist on the surface of the membranes. This proved to be difficult due to buckling of the membrane as it was either dried or absorbed solvent from the resist layer. The direct embossing of Nafion has the advantage of controlled surface modification without chemical contamination. Previously we observed that chemicals used in modern micromachining processes (e.g. photoresist, photoresist developer, solvent, etc.) can negatively impact the performance of an MEA [12]. Since lift-off and post-chemical treatment was not required for this process, a shadow mask was created to selectively deposit Pt over the embossed nanostructured features. For comparison, O'Hayre et al. reported a peak in performance for Pt sputtered thin films (5–10 nm) on top of a smooth Nafion 117 surface [13]. The maximum power was several orders of magnitude higher than thinner or thicker films. Fig. 8 illustrates a 7.5 nm Pt film deposited on top of an embossed (nanostructured) Nafion 117 surface. The imprinted patterns were consistent with the Nafion thin films shown in Fig. 6.

The membrane was fabricated into an MEA and the performance was compared to an MEA prepared using conventional materials. The polarization curves are illustrated in Fig. 9. Although the peak power density of the nanoimprinted MEA was 123 mW cm^{-2}, which was lower than that for the conventionally prepared MEA (410 mW cm^{-2}), the Pt utilization for the former was 15,375 mW mg^{-1} Pt compared to 820 mW mg^{-1} Pt for the conventional electrode. These values were determined by dividing the peak power density by the Pt loadings for the anode (conventional MEA, 0.5 mg cm^{-2}; MEA with nanoimprinted electrode, 8 μg cm^{-2}). Further characterization of the Pt on the nanoimprinted Nafion is underway and will be presented in a follow-up paper. The added areas from the Pt on the sidewalls of the nanostructures could contribute to increased performance over a planar surface. For instance for the structure used in this study (Fig. 2A), the available added surface area is twice the amount of the planar surface. The improvement of a Pt film deposited onto Nafion achieved with this method is also consistent with improvements demonstrated by Cha et al. In this work, MEAs with sputtered films of Pt (deposited on top of the catalyst layer) showed an increase in performance compared to standard MEAs [14]. The conclusion was that a higher concentration of Pt either near the GDL or Nafion layers increased performance of the catalyst layer.

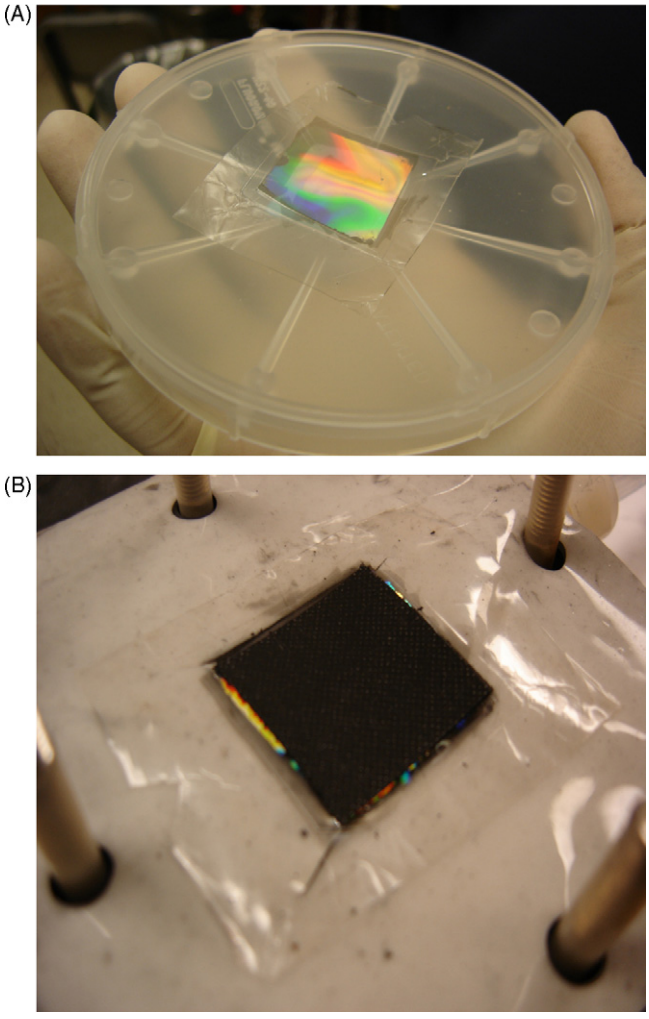

Fig. 8. (A) Illustration of Pt on embossed Nafion 117 film; (B) embossed Nafion 117 MEA.

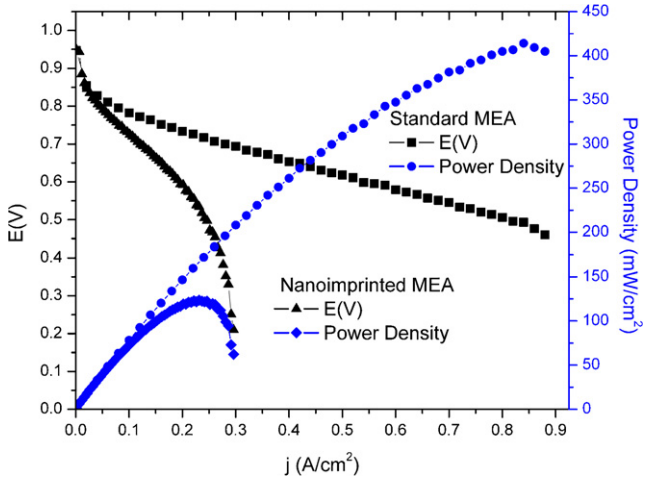

Fig. 9. Polarization curves of standard MEA and nanoimprinted MEA.

4. Discussion

In order to improve the performance of micro-fuel cells, there will need to be an increase in the EAS area. This observed difference in EAS values (between standard Pt/C catalysts and Pt thin films) is directly related to overall fuel cell performance. In the micro-fuel cell research highlighted by Nguyen and Chen, it can be observed that the peak power densities of thin film electrode micro-fuel cells show lower (several orders of magnitude) performance compared to micro-fuel cells made with conventional catalysts [15]. Thin film electrodes that are CMOS compatible offer the possibility of fabricating the entire system using standard micromachining techniques. As a result, we believe that the same cost advantages realized in the integrated circuit industry could translate into reduced costs for fuel cells. The micro-fuel cells could also be fabricated with control circuitry and other electronic components which is not presently possible with lithium ion batteries.

Although circumventing the 2D characteristics of existing catalyst deposition techniques (i.e. sputtering, e-beam evaporation) would be attractive, a low cost method may exist where nanoimprinting could play an important role. For example, the control of catalyst particle size and orientation through the use of NIL could be a useful way to construct model catalysts. In addition, with the precise control of thin film thickness available using micromachining facilities coupled with smaller feature sizes available from NIL, the exploitation of unique material properties available at the nanoscale could be further realized.

5. Summary

In summary, we have fabricated electrodes with Pt nanostructures using the NIL method. The Pt nanostructures were active for hydrogen oxidation and the material was polycrystalline. We also demonstrated a simple method of embossing nanostructures directly onto Nafion thin films which could be used for the next generation MEMs (microelectromechanical systems) devices exploiting the material properties of an ion-selective membrane. An embossed Nafion 117 film with Pt deposited on the nanostructures was fabricated into an MEA and demonstrated to be active. The catalyst layer on the embossed nanostructured Nafion had a significantly higher Pt utilization than a conventional catalyst layer.

Acknowledgements

This study was supported in part by a faculty seed grant awarded to André D. Taylor by the Office of the Vice President for Research at the University of Michigan. Financial support from the Hydrogen Energy Technology Laboratory is also appreciated. We would like to thank Brendan Casey of the Wireless Integrated Microsystems (WIMS) Center for wirebonding and connecting the electrodes that were tested.

References

[1] S.C. Kelley, G.A. Deluga, W.H. Smyrl, AIChE J. 48 (2002) 1071–1082.
[2] G.Q. Lu, C.Y. Wang, T.J. Yen, X. Zhang, Electrochim. Acta 49 (2004) 821–828.
[3] J.P. Meyers, H.L. Maynard, J. Power Sources 109 (2002) 76–88.
[4] R. O'Hayre, T. Fabian, S.J. Lee, F.B. Prinz, J. Electrochem. Soc. 150 (2003) A430–A438.
[5] J.D. Morse, A.F. Jankowski, R.T. Graff, J.P. Hayes, J. Vac. Sci. Technol. A: Vac. Surf. Films 18 (2000) 2003–2005.
[6] A.D. Taylor, L.T. Thompson, IEEE Solid State Sensors and Actuators Workshop, Hilton Head, South Carolina, 2004.
[7] R.S. Jayashree, J.S. Spendelow, J. Yeom, C. Rastogi, M.A. Shannon, P.J.A. Kenis, Electrochim. Acta 50 (2005) 4674–4682.
[8] L.J. Guo, J. Phys. D: Appl. Phys. 37 (2004) R123–R141.
[9] S.Y. Chou, P.R. Krauss, L.S. Kong, J. Appl. Phys. 79 (1996) 6101–6106.
[10] L.R. Bao, X. Cheng, X.D. Huang, L.J. Guo, S.W. Pang, A.F. Yee, J. Vac. Sci. Technol. B 20 (2002) 2881–2886.
[11] T.R. Ralph, G.A. Hards, J.E. Keating, S.A. Campbell, D.P. Wilkinson, M. Davis, J. St. Pierre, M.C. Johnson, J. Electrochem. Soc. 144 (1997) 3845–3857.
[12] A.D. Taylor, L.T. Thompson, in preparation.
[13] R. O'Hayre, S.-J. Lee, S.-W. Cha, F.B. Prinz, J. Power Sources 109 (2002) 483–493.
[14] S.Y. Cha, W.M. Lee, J. Electrochem. Soc. 146 (1999) 4055–4060.
[15] N.T. Nguyen, S.H. Chan, J. Micromech. Microeng. 16 (2006) R1–R12.